TOMOGRAPHIC IMAGE RECONSTRUCTION OF FAN-BEAM PROJECTIONS WITH EQUIDISTANT DETECTORS USING PARTIALLY CONNECTED NEURAL NETWORKS

Luciano Frontino de Medeiros
FACINTER/PR
lfm@netpar.com.br
Hamilton Pereira da Silva
COPPE/UFRJ
hps_curitiba@yahoo.com
Eduardo Parente Ribeiro
UFPR
edu@eletrica.ufpr.br

Abstract: We present a neural network approach for tomographic imaging problem using interpolation methods and fan-beam projections. This approach uses a partially connected neural network especially assembled for solving tomographic reconstruction with no need of training. We extended the calculations to perform reconstruction with interpolation and to allow tomography of fan-beam geometry. The main goal is to aggregate speed while maintaining or improving the quality of the tomographic reconstruction process.

Index Terms: Tomography, reconstruction, neural network, fan-beam, interpolation.

1. Introduction

Neural networks have already been studied for tomographic image reconstruction using multilayer perceptron with backpropagation training methods [1-3]. Self-organizing neural networks have also been proposed to reconstruct original image when a limited number of projections is available [4]. In this article, we present an alternative approach to obtain computerized tomography (CT) images using partially connected neural networks whose synaptic connections are calculated according to the geometry of problem without the need of training. We have extended the formulation of early works [5,6] to include interpolation and fan-beam geometry. This configuration is more closely related to the one used on most equipments where a single x-ray source emits a thin divergent beam and several detectors receive the radiation after attenuation by the object [7]. If the distance between source and detectors is large enough, the rays can be considered parallel and tomographic reconstruction assuming parallel rays will produce negligible errors. On the other hand, if the distance is small, the angles between source and detectors will be representative resulting in a distorted reconstructed image. In figure 1, a simulation with a synthetic *Sheep-Logan* phantom was performed to illustrate such effect. If the x-ray measurements were made assuming parallel geometry the reconstruction with the same model results in a good image (a) but if the detectors were positioned in a fan-beam fashion the same reconstruction with parallel geometry would provide an image with undesirable artifacts.

Reconstructed image quality can also be improved by using linear interpolation instead of simple truncation which is what is usually done due to the discrete processing of data. We show how interpolation can be naturally incorporated to network weights to produce the desired reconstructed image. The proposed partially connected neural network has its weights previously calculated according to the geometry of the problem including interpolation. This weighed filtered backprojection implementation can be calculated faster than convention reconstruction with the expense of more memory usage to store the weights [8]. Hardware implementation of such network could better explore the inherent parallelism of the problem and achieve a very significant speedup [9].

2. Methods

A tomographic projection of an object is obtained when an electromagnetic radiation beam (like x-ray or gamma ray) pass through the object and projects a shadow in a fence or image intensifier at the opposite side (figure 2). Object essentials properties like mass rest or specific density raise a resistance, reducing the intensity of the beam, which decays exponentially according to the total radiopacity along the path of the ray [10,11]:

$$I = I_0 \exp\left\{-\int_L f(x, y)du\right\} \tag{1}$$

where $f(x,y)$ represents the absorption coefficient at a point (x,y), L is the path of the ray and u is the distance along L.
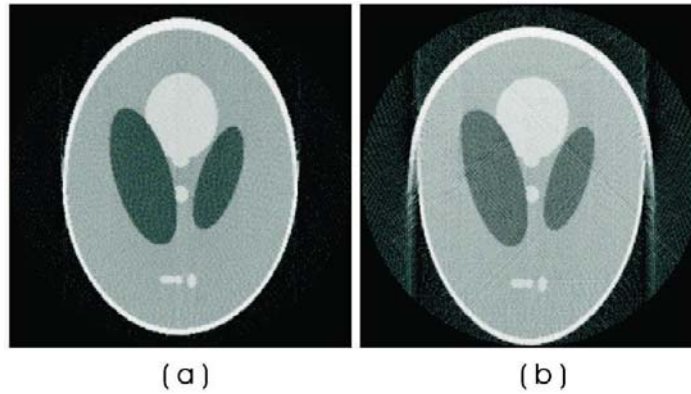
Figure 1: Reconstructed images from projections of the same synthetic phantom (Shepp-Logan) using parallel beam reconstruction geometry. (a) Projections generated by parallel beam. (b) Projections generated by fan-beam (more realistic) geometry lead to distorted image when parallel beam reconstruction is used.

Measuring the logarithm of the intensity ratio at different positions (*s*) for several angles (*θ*) leads to

$$p(s,\theta) = \ln\left(\frac{I_0}{I}\right) = \int_L f(x,y)du \qquad (2)$$

The pair (s,θ) represents the ray coordinates related to the object. *s* is the shift from the center and *θ* the angle at which the measurement is obtained. The values $p(s,\theta)$ form a image that is the projection obtained from these external measurements. This image is also called sinogram because a single point in the object ($f(x,y)$) is mapped to a sinusoid in this projection space.

The reconstruction problem is to obtain $f(x,y)$ from the projection $p(s,\theta)$.
The Radon transform describes the direct problem or projection generation process. The inverse problem, or reconstruction process can be calculated by the inverse Radon transform, but this is seldom used due to its complexity:

$$f(r,\phi) = \left(\frac{1}{2\pi^2}\right)\int_0^\pi \int_{-\infty}^{+\infty} \frac{\partial p(s,\theta)/\partial s}{r\cos(\theta-\phi)}dsd\theta \qquad (3)$$

where (r,ϕ) are polar coordinates of the image to be reconstructed. It can be shown that $f(r,\phi)$ can also be calculated by backprojecting $q(s,\theta)$ a high-pass filtered version of $p(s,\theta)$ [10,11]:

$$\hat{f}(r,\phi) = \int_0^\pi q(r\cos(\theta-\phi),\theta)d\theta \qquad (4)$$

where the backprojection operation is simply the accumulation of the ray-sums of all the rays that pass through the point (r,ϕ). Most equipments use filter backprojection as the reconstruction algorithm, because it is easier to calculate. Among other methods less used are Fourier Reconstruction and ART (Algebraic Reconstruction Techniques).
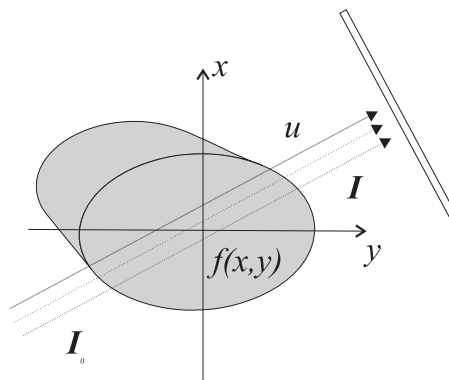

Figure 2: Radiation beam crossing an object, producing a "shadow" over the plate at the right-upper of figure.

Figure 3: Geometric representation of projections with parallel beans.

Figure 3 illustrates the geometry of the problem for the parallel beam crossing the object yielding a profile over the detectors line-arrange. Ideally, the detector at point A measures the amount of radiation due to only one ray yielding a projection quantity $p(s,\theta)$, also called ray-sum for that point. The angle between *OA'* segment and the *x*-axis is θ (or equivalently the angle between ray direction and y-axis). The shift *s* corresponds to the *OA'* segment modulus, and can be expressed in terms of a generic point (r,ϕ) by the follow geometric relationship:

$$s = r\cos(\theta - \phi) \tag{5}$$

This relation has fundamental importance in the tomographic reconstruction process, showing that the relationship between projection and final image is *purely geometric*. It does not have any relation to the specific content of projections or the final image.

So far, the explanation of tomographic reconstruction was based on parallel ray beam crossing the object. Many equipments collect data in a fan-beam arrangement rather than parallel beam, allowing a single source of x-ray close to the object and rapid collection of projections. When dealing with fan-beam projections, the source ray is considered punctual. There are two kinds of fan-beam projections: *equidistant* and *equiangular* intervals between each detector along the line. In this article we focused on equidistant intervals configuration.

Figure 4 shows a source located at point *S*, from a certain distance *D* to the origin emitting divergent rays at angle β. The ray-sum at an angle β yields a projection value in the line detectors over the D_1D_2 segment. By transposing this line to an imaginary segment $D'_1D'_2$ the shift *s* related to the *OA'* segment can be computed by the expression [12],

$$s' = \frac{r\cos(\beta - \phi)}{U} \tag{6}$$

where *U* is a weighting factor expressed in terms of the source to origin distance *D*:

$$U = 1 + \frac{r\sin(\beta - \phi)}{D} \tag{7}$$

When *D* approaches infinity, *U* tends to unity and expression (6) will match expression (5). Therefore, when the source is positioned at a large distance from the object, fan-beam geometry will be equivalent to parallel ray beam geometry.
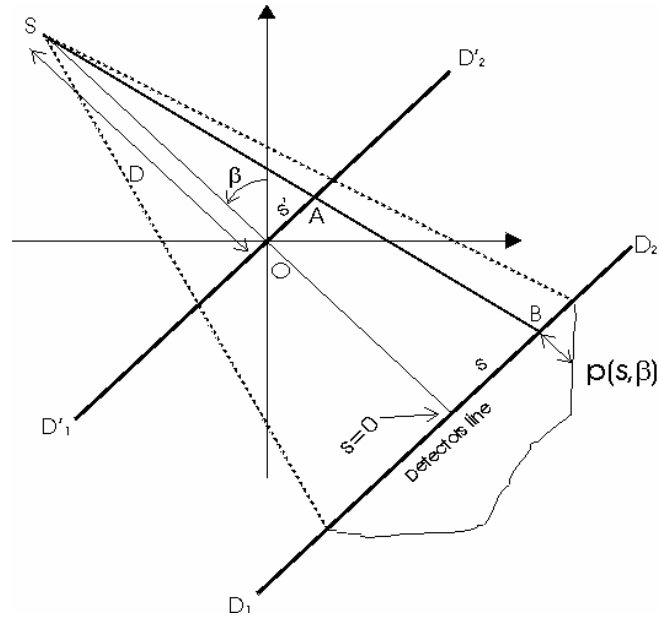
Figure 4: Geometric representation of projections given by fan-beam geometry.

In our approach, the filter backprojection is implemented by two partially connected neural networks with aim to make good use of parallelism supplied by this structure to provide more speed in the reconstruction process [5,6]:

1. Partially connected neural network for filtering
2. Partially connected neural network for backprojection.

Next, we describe the backprojection neural network and modifications needed for the CT reconstruction with fan-beam geometry.

2.1 Backprojection Network

The backprojection operation shown in equation (4) can be expressed for K discrete angle steps as:

$$\hat{f}(r,\phi) = \frac{1}{K} \sum_{k=1}^{K} q(r\cos(\theta-\phi),\theta_k) \tag{8}$$

where the θ_k are the angles obtained at constant intervals $\Delta\theta$. Each pixel in $\hat{f}(x, y)$ or in polar coordinate $\hat{f}(r,\phi)$ will be the summation of all ray-sums that had traversed that pixel. This represents the accumulation of the values along a sinusoid on the (s,θ) plane as shown in figure 5.
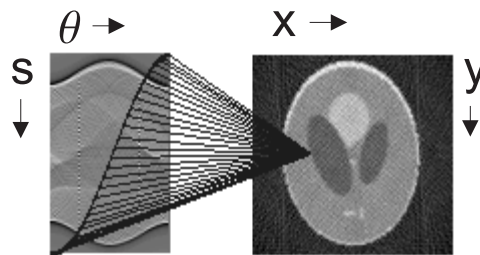
Figure 5: Backprojection process: contribution of (s, θ) pixels to a (x,y) pixel in the final image.

It was shown in previous works [5,6], that this equation can be implemented by a one layer feedforward network with its weights previously determined in terms of the geometry of the problem. The expression of a fully connected neural network with linear activation function is given by [13]:

$$y_j = \sum_{i=1}^{N} w_{ji} x_i \tag{9}$$

where each output y_j is connected to the input x_i with a weight w_{ji}. Comparing this expression with equation (8), allows one to rewrite the backprojections in terms of synaptic weights where each pixel in the final image are fully connected by weights w_{ij} to all pixels of q(s,θ). Index j enumerates all M pixels in the final image $f(r,\theta)$ while index i enumerates all N pixels in $q(s,q)$:

$$f(r,\phi) = y_j = \frac{1}{K}\sum_{i=1}^{N} w_{ji} x_i = \frac{1}{K}\sum_{i=1}^{N} w_{ji} q(s,\theta) \tag{10}$$

Note that some weights will be unity and others will be zero. To reduce memory usage and improve speed the null weights can be purged yielding a partially connected neural network.

Equation (8) can be slightly modified to take into account the fan-beam geometry (4) [8]:

$$f(r,\phi) = \frac{1}{K}\sum_{k=1}^{K} \frac{1}{U^2} q(\frac{r\cos(\beta_i - \phi)}{U}, \beta_i) \tag{11}$$

The neural network can be easily modified to incorporate this new scenario. The only change needed is on the weights values. Instead of unity their value should be given by

$$w_{ji} = U^{-2} \tag{12}$$
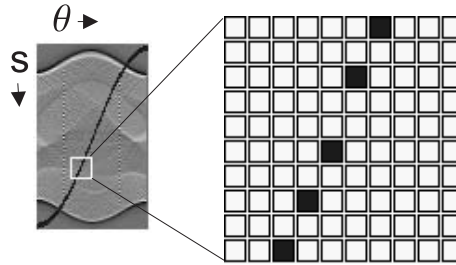
Figure 6: Zoom of part of the sinusoid, showing the points calculated according to the equation 4.

Another refinement to be incorporated in the reconstruction network is interpolation. When discretizing the calculated value of s which is a function of the angle θ as expressed in (4) the nearest pixel is selected. This way only a few relevant pixels in $q(s,\theta)$ will contribute to a given pixel in the final image. Figure 6 shows a zoomed view of the sinusoid relation in $q(s,\theta)$ where significant space between adjacent pixels can be seen. To improve image quality, we use the interpolation method [11,12] to make a good use of neighboring pixels. The procedure to obtain a linear interpolation is to compute a weighted combination of the two adjacent pixels according to proximity of them to the sinusoid. Figure 7 illustrates the adjacent pixels incorporated. Backprojection is then given by:

$$f(r,\phi) = \frac{1}{K}\sum_{k=1}^{K} [u_k\, q(\lfloor s \rfloor, \theta_k) + v_k\, q(\lceil s \rceil, \theta_k)] \tag{13}$$

where the calculated value of s is truncated downwards $\lfloor s \rfloor$ (floor of s) to the closest number in the discretized s axis, or truncated upward $\lceil s \rceil$ (ceil of s).

The weights u_i and v_i are calculated by

$$u_i = \lceil s \rceil - s = \lceil s \rceil - r\cos(\theta_i - \phi) \tag{14}$$

and

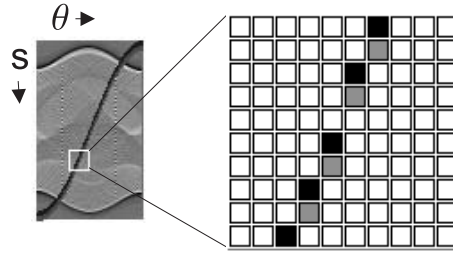$$v_i = s - \lfloor s \rfloor = r\cos(\theta_i - \phi) - \lfloor s \rfloor \tag{15}$$

Figure 7: Zoom of part of the sinusoid, now showing the points located at gaps (in gray) used in the interpolation method.

It is clear from the equations (16) and (17) that the weights are complementary themselves,

$$u_i = 1 - v_i \tag{16}$$

and both belong to the range [0,1].

The resulting single layer partially connected neural network to compute backprojection with fan-beam geometry and interpolation is:

$$f(r,\phi) = y_j = \frac{1}{K} \sum_{k=1}^{K} [u_{jk} \, q(\lfloor s \rfloor, \theta_k) + v_{jk} \, q(\lceil s \rceil, \theta_k)] \tag{17}$$

where the synaptic weights are given by:

$$v_{ji} = U^{-2}(\lceil s \rceil - s) \tag{18}$$

and

$$v_{ji} = U^{-2}(s - \lfloor s \rfloor) \tag{19}$$

It is worth mentioning that the backprojection algorithm using partially connected neural networks needs to run in two distinct phases: the *building* phase where the relevant weights are calculated and the *feeding* phase where the filtered projection is presented at the input and the values propagate to the output according to the weights giving the reconstructed image. The building phase involves the weights calculated by equations (14) and (15) for parallel beam, or equations (18) and (19) for fan-beam with interpolation geometry. The network structure is very similar, the main difference resides on the weights values. Network for parallel beam reconstruction with no interpolation have only unity weights while network with interpolation or fan-beam geometry have non-integer weight values.

2.2 Filtering Network
The high-pass filtering process required for the inverse Radon transform amplifies high spatial frequencies. To avoid excessive noise amplification at these frequencies a band-limited filter, called Ram-Lak filter is often used [10,11,14]. The filter impulse response is:

$$h(n) = \begin{cases} \tfrac{1}{4}, & n = 0 \\ 0, & n \text{ even} \\ \dfrac{-1}{n^2 \pi^2}, & n \text{ odd.} \end{cases} \tag{20}$$

Only the first N values of n are considered, and the resulting FIR (finite impulse response) filter can be calculated by convolving the filter impulse response with the input data, in this case the projection image $p(s,\theta)$. This convolution operation is implemented as a single layer neural network with linear activation function according to previous works [5,6].

$$q(n,\theta) = \sum_{k=1}^{N} h(n-k) \, p(s_k, \theta), \qquad n = 1,..,N$$

For fan-beam geometry, the projections (in this case named *p'*) need to be multiplied by an adjust function, before the filter [7]:

$$p(n,\theta) = p'(n,\theta)\frac{D}{\sqrt{D^2 + n^2}} \tag{21}$$

After the compensation, the convolution is carried out with a slight modification in the filter coefficients:

$$h(n) = \begin{cases} \frac{1}{8}, & n = 0 \\ 0, & n \text{ even} \\ \frac{-1}{2n^2\pi^2}, & n \text{ odd.} \end{cases} \tag{22}$$

The full reconstruction process consists on the two neural networks (*filtering* and *backprojection*) connected in cascade. The output of filtering network is connected to the input of backprojection network. This can also be seen as a single two-layer neural network and it could be implemented in an appropriate neural hardware.

3. Results

The proposed neural network was implemented in C++ and executed in a sequential processor for verification purposes. We compared the times for reconstruction with and without interpolation (and fan-beam). The experiment was run on a microcomputer with Pentium 1.6 MHz processor. The times were obtained from an average of 1000 algorithm runs. Table 1 lists the execution times for conventional backprojection algorithm and for neural network where the time to build the network (calculate the weights) and the time to process the reconstruction were measured separately.

	conventional backprojection		partially connected neural network			
	parallel	fan-beam	parallel		fan-beam	
			build	run	build	run
no interpolation	293	512	250	57	524	57
with interpolation	369	707	347	108	656	108

Table 1 – Execution times (in milliseconds) for neural network and
conventional backprojection reconstruction of images with 100x100 pixels

Total time to reconstruct one image is greater for neural network but once the network has been assembled the time to compute the reconstruction is very small. Network approach has noticeable advantages when several sections from an object need to be reconstructed in sequence, like in a 3-D representation. For example, reconstruction of 10 slices by conventional backprojection with fan-beam geometry would take 5.1s while the network would be constructed once and executed 10 times in 1.1s, almost 5 times faster.
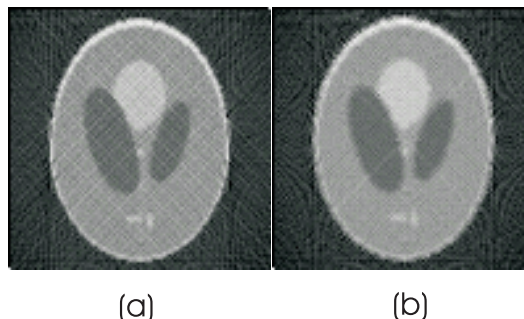

(a)   (b)

Figure 8: Sheep-Logan phantom reconstructed with dimension 100x100 by neural network, (a) without interpolation and (b) with interpolation.

In figure 8 reconstructed images without (a) and with (b) interpolation are shown. When interpolation is used a smother image with less artifacts is achieved. To compare image quality we computed its peak signal to noise ratio (PSNR) defined as the peak amplitude of the original phantom divided by the difference between original phantom and reconstructed image expressed in dB. Figure 9 shows a plot of PSNR as a function of the number of (FIR) filter coefficients use in the

filtering network. When more coefficients are used the FIR filter approaches the IIR (infinite impulse response) ideal filter and a better quality reconstruction results. In practice there is a limit after which no improvement is noticed in quality. Using more coefficient than that leads to a slight decrease in PSNR. Reconstruction with interpolation results in higher PSNR meaning better quality when more than 50 coefficients are used
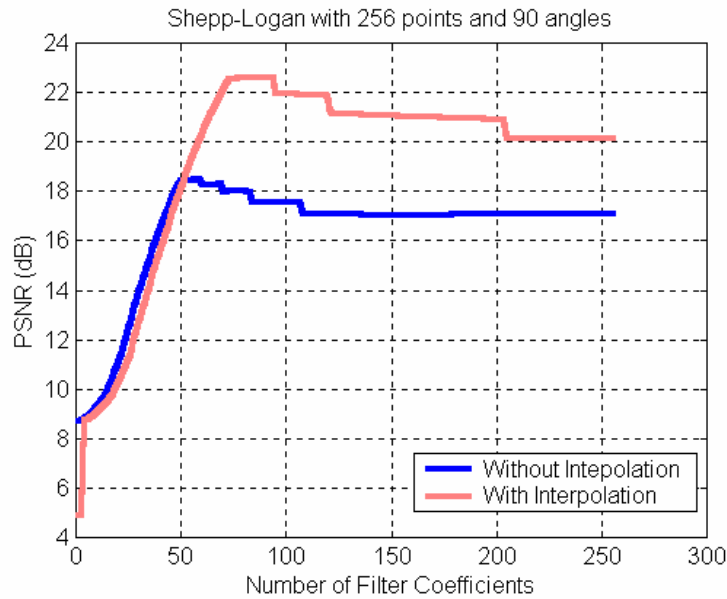

Figure 9: Plot of PSNR values versus number of (FIR) filter coefficients, showing that the best image quality is obtained using interpolation.

The following simulation was carried out to verify the influence of fan-beam geometry in the reconstruction process. The projection of Shepp-Logan synthetic phantom was generated assuming a fan-beam configuration with the ray source located D=20 units apart from origin. This sinogram was reconstructed by a neural network assembled for parallel geometry and by another network build for fan-beam geometry. The reconstructed images with 256x256 pixels had their PSNR computed and plotted for different distances D used to build the fan-beam reconstruction network. Figure 10 shows the resulting points and a polynomial fit to help the visualization of the region of maximum PSNR. This maximum quality is obtained when reconstruction if performed for values of D close to 20 units as expected.
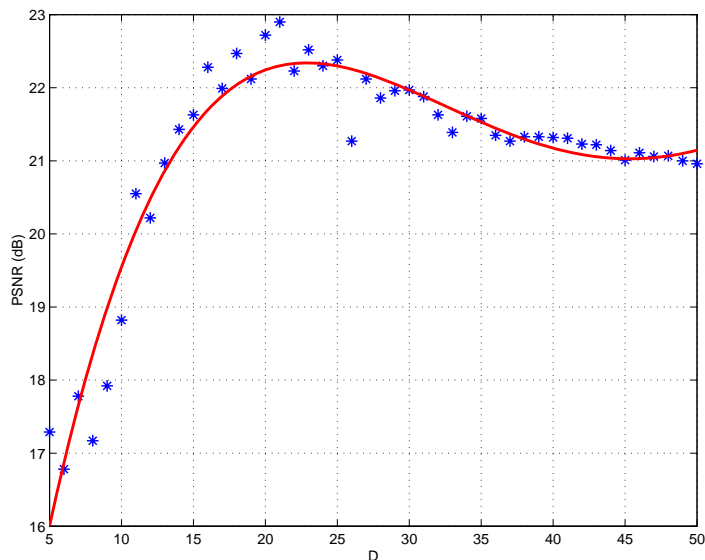

Figure 10: Plot of PSNR values of reconstructed image under the geometry fan-beam with distance D varying at defined range.

129

4. Conclusion

It was presented a different approach for tomographic reconstruction process involving neural network. Calculations to include fan-beam geometry and interpolation were adapted for this approach. The proposed partially connected neural network doesn't need to be trained and its weights are previously calculated according to the geometry of the problem. The relationship between the projection space and final image is purely geometric not only for parallel beam but also for fan-beam configuration. Once image size and number of projections are determined the network can be assembled and any tomographic image can be reconstructed from its projections presented to the network input.

Preliminary simulations on sequential processor showed 4 to 5 times speed-up in the reconstruction of 10 slices compared to conventional backpropagation algorithm. This technique is sought to be very advantageous for neural parallel hardware implementation where it will reach extremely high speed which is well desired for multi-slice reconstruction and real time tomography.

References

[1] M.T. Munley et al. *An artificial neural network approach to quantitative single photon emission computed tomographic reconstruction with collimator, attenuation and scatter compensation.* Med. Physics. 21 (12) (1994).

[2] J. P. Kerr and E. B. Bartlett. *A statistical tailored neural network approach to tomographic image reconstruction.* Med. Physics. 22(5) (1995).

[3] R. G. S. Rodrigues. *Desenvolvimento e Aplicação de um Algoritmo de Reconstrução Tomográfica com Base em Redes Neurais Artificiais.* Doctorate thesis. Faculdade de Filosofia, Ciências e Letras de Ribeirão Preto, SP (2000).

[4] H. Monma, Y. Chen, Z. Nakao. *Computed Tomography base on a Self-organizing Neural Network,* IEEE SMC '99 Conference Proceedings. (1999).

[5] L. F. Medeiros, H. P. da Silva and E. P. Ribeiro. *Reconstrução de Imagens Tomográficas utilizando Redes Neurais Parcialmente Conectadas.* Proceedings of the V Brazilian Conference of Neural Networks. Rio de Janeiro, RJ (2001).

[6] L. F. Medeiros. *Reconstrução de Imagens Tomográficas com Redes Neurais Parcialmente Conectadas.* Dissertação de Mestrado. UFPR. Curitiba, PR (2001).

[7] A. Rosenfeld and A. Kak. *Digital Picture Processing.* Academic Press. San Diego (1982).

[8] L. F. Medeiros, H. P. da Silva and E. P. Ribeiro. *Reconstrução de Imagens Tomográficas Geradas por Projeções Fan-Beam com Detectores Eqüidistantes usando Redes Neurais Parcialmente Conectadas.* Proceedings of the VI Brazilian Conference of Neural Networks. São Paulo, SP (2003).

[9] P. Williams, T. York. *Hardware implementation of RAM-based neural networks for tomographic data processing.* IEE Proceedings of Computers and Digital Techniques, pp. 114-118, (1999).

[10] A. K. Jain. *Fundamentals of Digital Image Processing.* Prentice-Hall, pp.431-475 (1989).

[11] G. T. Herman. *Image Reconstruction from Projections.* Academic Press, pp.90-160 (1980).

[12] G. T. Herman., S. W. Rowland and M. M. Yau. *A comparative study of the use of linear interpolation and modified cubic spline interpolation for image reconstruction.* IEEE Transactions Nuclear Sciences, pp.2879-2894 (1973).

[13] S. Haykin. Neural Networks – *A Comprehensive Foundation.* MacmillanColl. Pub. Com. Inc. pp.1-41 (1994).

[14] A. Kak and M. Slaney. *Principles of Computerized Imaging.* IEEE Press. New York (1988).